中國機械工程學刊第四十二卷第四期第 371~380 頁(民國一百一十年)
Journal of the Chinese Society of Mechanical Engineers, Vol.42, No.4, pp. 371~380 (2021)

The Effect of Downtime on Non-inertial Stopping Performance under Special Working Conditions

Yan-Juan Zhao*, Yu-Liang Zhang**, *** and Feng-Lin Zhou***

Keywords: self-priming pump, shut-off condition, non-inertial, transient performance, dimensionless analysis.

ABSTRACT

In this study, the non-inertial stopping behavior of a self-priming pump under shut-off and ultra-small-flowrate conditions is experimentally investigated, and the effect of downtime on such behavior is also examined. Transient characteristics in the non-inertial stopping process are deeply revealed through a dimensionless analysis. Results show that the non-inertial stopping process is prone to drop delay of rotating speed at the end of this process when the downtime is short. The non-inertial stopping process is prone to flowrate sudden drop at the end of this process when the downtime is long. Moreover, drop lag in flowrate is a common phenomenon in the early stage of the non-inertial stopping process. The three dimensionless coefficients have the minimum values in the early stage of the non-inertial stopping process then remain approximately unchanged and rapidly increase to the maximums at the end of the stoppings. The extent to which parameters are affected in the non-inertial stopping process is from heavy to light in the order of the head, shaft power, and flowrate. The similarity law of pump can be applied to the performance prediction of transient operating processes with long downtime.

Paper Received June, 2019. Revised September, 2019. Accepted October, 2020. Author for Correspondence: Yu-Liang Zhang.

* *College of Information Engineering, Quzhou College of Technology, Quzhou 324000, China.*

** *College of Mechanical Engineering & Key Laboratory of Air-driven Equipment Technology of Zhejiang Province, Quzhou University, Quzhou, 324000, China.*

*** *School of Mechanical Engineering, Hunan University of Technology, Zhuzhou, 412007, China.*

INTRODUCTION

Centrifugal pumps are a type of widely used fluid conveyor. All types of pump units generally operate stably in a state with an approximate constant rotating speed, but some transition processes, such as sudden start-up and power outage, are inevitable. In the rapid start-up of the rocket turbine pump and accidental power outage of the nuclear main pump in a nuclear power plant, good mastery of transient performance is necessary to ensure the safe and reliable operation of the entire equipment. Many scholars have performed theoretical analyses, numerical calculation, and experimental study of various transition processes of pumps and other hydraulic devices, such as pump sudden start-up (Tsukamoto et al., 1982; Lefebvre et al., 1995; Thanapandi et al., 1994,1995; Duplaa et al., 2010; Li et al., 2010; Zhang et al., 2014a, 2016, 2017b, 2018a; Dazin et al., 2007; Tanaka et al., 1999; Rong et al., 1996; Gao et al., 2013), pump stopping (Thanapandi et al., 1994, 1995; Zhang et al., 2014a, 2016, 2017a, 2018a, 2018b; Tanaka et al., 1999; Rong et al., 1996; Tsukamoto et al., 1986; Liu et al. , 2011; Wu et al., 2014; Gao, 2011; Chen , 2006; Wang, 2013; Zou, 2019; Wu et al. , 2017), rapid flowrate regulation of pump (Tanaka et al., 1999; Wu et al., 2010; Wu et al., 2010; Wu et al., 2010; Zhang et al., 2014b), rapid adjustment of the pump rotating speed (Wu et al., 2010; Zhang et al., 2014b). Numerical calculation includes the performance prediction of external characteristic and the numerical simulation of internal flow field and experimental researches includes the performance testing of external characteristics and the visualization of the internal flow field.

It is found from above-mentioned representative studies that these researches focus on the inertial stopping process of centrifugal pumps. The so-called inertial stopping processes refer to the capability to rely on rotor inertia to maintain continuous rotation, namely that no external force plays a role in controlling rotational speed. In other words, the declining rotational speed thoroughly depends on the rotor inertia. In nuclear power plants, during

unexpected power failure in extreme operating conditions, the nuclear main pump must rely on its own inertia to maintain continuous operating, and provide sufficient flowrate of the working medium for removing the waste heat of the reactor core, and ensure the safety of nuclear power plants. The performance of the nuclear main pump in the inertial stopping process is crucial in nuclear reactors.

The aforementioned studies, including the author's previous work (Zhang et al., 2012, 2016, 2018d), show that most of the existing researches on the stopping process of centrifugal pumps is based on the inertial stopping process. In the author's latest study (Zhang et al., 2017a, 2018a), the stopping hydraulic characteristics of a pump model were investigated based on the linear descent law of the given rotating speed. This study is different from the inertial stopping process, which is a typical non-inertial stopping process. Comparing with the traditional inertial stoppings, the research on non-inertial stopping processes is relatively few. Moreover, it is also easy to found that in non-inertial stopping process, the rotational speed is actively controlled to decline according to a certain rule through giving certain external force. The advantages of non-inertial and inertial stopping processes are controllable rotational speed and no external force, respectively. The disadvantages of both are required external force and uncontrollable rotational speed, respectively.

As we know, hump phenomenon often occurs under small flowrate conditions. As such, the operating of pump would become unstable. Therefore, it is very necessary to deeply master the transient hydraulic performance of pump during non-inertial stopping periods under small flowrate condition so as to avoid serious operating problem.

In this paper, the non-inertial stopping behaviour of a pump model under the conditions of shut-off and ultra-small flowrate points, in which the initial flowrates before non-inertial stopping are 0.0 m^3/h and 4.0 m^3/h, respectively, are discussed and revealed. The shut-off and ultra-small-flowrate conditions are special working condition for a certain pump.

Thus far, the hydraulic characteristics of a pump in the non-inertial stopping process are far from being mastered. Hence, the study sets the drop time and descent law of the output current intensity through a frequency conversion controller to actively control the drop characteristics of rotating speed and realize the non-inertial stopping process. The opening of discharge valve at pump outlet is controlled to actively control the stable flowrate before stoppings. In this paper, two stable working conditions, namely, shut-off and ultra-small-flowrate, occur before stoppings. Under the shut-off condition, the discharge valve is completely closed, and therefore the passing flowrate is zero. Both of these working conditions are special cases for pump. The transient hydraulic performance in non-inertial stopping process is determined through experiments, and the transient characteristics of the tested pump in the non-inertial stopping process are deeply revealed through a dimensionless analysis. In short, the main contribution of the paper is to master the non-inertial stopping characteristics under two special operating conditions by means of external performance experiments.

PHYSICIAL PUMP AND TEST RIG

Tested Pump

The test pump used in this study is a DKS18-40-3 cantilever type self-priming centrifugal pump. Its designed rotating speed, flowrate, and head are 2,900 r/min, 10 m^3/h, and 35 m, respectively. The pump inlet diameter, pump outlet diameter, impeller inlet diameter, impeller outer diameter, blade inlet width, exit width, blade inlet angle, and blade outlet angle are 60 mm, 60 mm, 40 mm, 166 mm, 8 mm, 8 mm, 40°, and 20°, respectively. Figure 1 shows the internal structure of the self-priming pump.

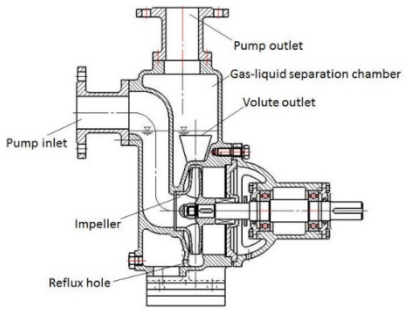

Fig. 1. Section view of self-priming.

Test Rig

The test rig of pump external performance during non-inertial stopping process is shown in Figure 2. The model types, measuring ranges, and measurement accuracy of each measuring sensor are exactly the same as those in previous study (Zhang et al., 2016). A torque detector of type JC0 with the range of 0~20 N.m is adopted to measure the instantaneous rotational speed and shaft power with the total uncertainty of ±0.65% in them. An electromagnetic flowmeter of type OPTIFLUX2100C with the range of 0~30 m^3/h is utilized to measure the instantaneous flow rate with an uncertainty of ±0.5%. Two pressure transmitters of type WIKA S-10 are used to monitor the instantaneous pressures at the pump inlet and outlet with the ranges of (-0.1~1.0) MPa and (0~1.6) MPa, respectively and the uncertainty of ±0.75%. The measurement accuracy is less than 0.25% in both transmitters. The conveying medium is clear water at room temperature. Its density is 998.2 kg/m^3, and its dynamic viscosity is $1.0069 \times 10{-}3pa{\cdot}s$.

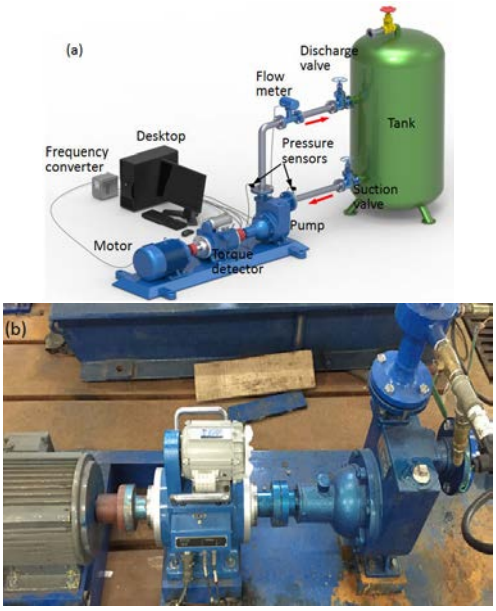

Fig. 2. Test rig (a) schematic diagram (b) tested pump unit.

Testing Method and Scheme

The drop time and descent law of the output current intensity are set through the frequency conversion controller to actively control the drop characteristics of rotating speed. At a rated voltage of 220 V, the maximum frequency of current is 50 Hz, and the corresponding maximum rotating speed in theory is 2,900 r/min. The actual initial value shows a slight fluctuation due to voltage fluctuations and other reasons. In this paper, the output current is linearly reduced, and therefore the pump rotating speed is also linearly reduced to zero theoretically. The time required for downtime is set to 1.0, 3.0, 5.0, 7.0, and 9.0 s, which are defined as the five non-inertial stopping states of ultrafast, rapid, moderate, slow, and superslow, respectively.

The valve opening of discharge valve at pump outlet is controlled to regulate the stable conveying flowrate before stoppings. In this study, two kinds of openings, namely, zero opening and small opening, are set, and they correspond to stable flowrates of 0.0 and 4.0 m^3/h under shut-off and ultra-small flowrate conditions. Table 1 shows the specific test scheme in the non-inertial stopping process in this study.

Before the test, the entire circulating piping system is filled with water, and the free liquid surface of the water tank is always higher than that of the test pump and the whole piping system. The discharge valve is completely closed in advance under the shut-off condition. Subsequently, the pump unit is activated, and the non-inertial stopping experiments are carried out after the rotating speed reaches the designed value and stabilizes to complete the five types of non-inertial stoppings in Table 1. For the ultra-small flowrate condition, the pump unit is initially activated. After reaching the designed rotating speed and stabilizing, the discharge valve opening is repeatedly adjusted to obtain stable flowrate of 4.0 m^3/h. The discharge valve opening is unchanged. At this moment, the drop time and drop law of the output current are set in the inverter. Subsequently, the non-inertial stopping experiments are performed to obtain the transient performance curve of the pump during non-inertial stopping periods.

Table 1. Testing schmes.

Testing case	No.1	No.2	No.3	No.4	No.5
The defined state	ultrafast	rapid	moderate	slow	superslow
Drop time of rotating speed(t/(s))	1.0	3.0	5.0	7.0	9.0
Initial flowrate before stopping(Q/(m^3/h))	0,4				

EXPERIMENTAL RESULTS

Rotating speed characteristics

Figure 3 shows the instantaneous rotating speed of pump in the non-inertial stopping process measured by a JC0 torque speed sensor. In this experiment, the average initial rotating speeds under the shut-off and ultra-small-flowrate conditions are approximately 2,952 and 2,943 r/min, respectively. The rotating speeds show small drop characteristics with the increase in initial stable flowrate. The reason for small drop characteristics could be explained through flow theory of pump, namely that as the stable flowrate before stoppings increases, the shaft power would increase, which in turn increases the motor load, resulting in decreasing the output rotating speed of the motor (i.e., the pump rotating speed decreases). Meanwhile, it is seen that the initial rotational speeds are higher than 2,900 r/min, this is because the voltage is slightly higher than 220 V during the experiment.

In this experiment, the output current of the inverter controller is set to decrease linearly. Therefore, in theory, the pump rotating speed is also reduced to zero according to the linear law. The test results in Figure 3 show that the rotating speed in the states of moderate, slow, and superslow, which are the three stopping states, is basically reduced according to the linear law. This result is consistent with the expected value of rotating speed drop. However, the decrease in rotating speed at the end of the non-inertial stopping process for ultrafast and rapid states, which are the two types of stopping, deviates from the linear law, and the decrement rate decreases with a delay in the speed drop; the delay is particularly noticeable in the ultrafast state. This finding fully shows that the shorter the downtime is, the greater the speed acceleration is and the more difficult it is to control the rotating speed change.

For the shut-off state of 0.0 m^3/h, the rotating speeds under the five types of stopping (downtime from short to long) drop to zero, that is, the time required for the impeller to completely stop rotating is approximately 1.578, 3.312, 5.219, 7.203, and 9.141 s. Similar to the shut-off state, the total time required for the impeller to stop rotating completely in the ultra-small-flowrate state of 4.0 m3/h is approximately 1.531, 3.343, 5.203, 7.219, and 9.109 s. It is easy to found that the actual downtime is higher than the theoretical set time of 1.0, 3.0, 5.0, 7.0, and 9.0 s. The reason is that when the current drops to zero, the rotating inertia of the impeller, the liquid in the impeller, and the flow inertia of the liquid in the pipe make the impeller continue to rotate, thereby prolonging the impeller rotation process.

It is observed that the resultant curves for shut-off and ultra-small flowrate conditions are almost the same. In authors' previous work (Zhang, 2016), the similar results are also observed. This is attributed to that the decline characteristic of rotating speed is actively controlled by the frequency converter, namely that the declining rule of the rotational speed has nothing to do with the working conditions or has less relevancy during non-inertial stopping periods.

For the shut-off state and under the ultrafast and rapid states, the time inflection points at which the speed drop rate is significantly reduced are approximately 1.10 and 3.05 s, respectively, and the corresponding instantaneous rotating speeds are about 150 r/min and 75 r/min, respectively. For the ultra-small-flowrate state and above two types of stopping states, the time inflection points at which the speed drop rate significantly decreases are approximately 1.10 s and 3.0 s, respectively, and the corresponding instantaneous rotating speeds are approximately 120 and 110 r/min, respectively. It is not difficult to see that for the ultrafast stopping state, the time of the inflection point of the rotating speed drop lags behind the set time of 1.0 s, whereas in the rapid stopping state, the time at which the rotating speed drop occurs is approximately 3.0 s. This phenomenon indicates that the shorter the downtime is, the more likely the rotating speed drop is to show an inflection point.

In this paper, the parameter attenuation feature time is defined as the time that a parameter goes through when it drops to 36.8% of the initial value. In this study, the ratios (λ_n) of the attenuation characteristic time (t_n) of rotating speed to the total time (T_n) required for the impeller to stop turning show obvious differences. For the shut-off state, the rotating speed attenuation time ratios (λ_n) in the five types of stopping are approximately 0.463, 0.607, 0.623, 0.623, and 0.629. For the ultra-small-flowrate state, the rotating speed attenuation time ratios (λ_n) in the five types of stopping are approximately 0.475, 0.595, 0.625, 0.620, and 0.626. The rotating speed attenuation time ratio (λ_n) is further confirmed, except that a delay is observed in the end of ultrafast stopping process, whereas no delay is observed in other stopping states.

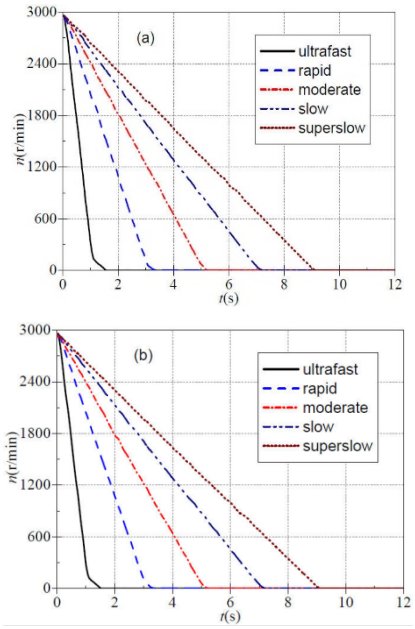

Fig. 3. Instantaneous rotating speeds (a) Q_i=0 (b) Q_i=4 (m^3/h).

Flowrate Characteristics

The instantaneous flowrate in the process of non-inertial stopping measured by an OPTIFLUX2100C electromagnetic flowmeter is shown in Figure 4. For the shut-off state, the discharge valve is completely closed, and the passed flowrate is zero. Therefore, only the instantaneous flowrate under the ultra-small-flowrate condition are shown in Fig. 4. In this study, the tested stable flowrate are all 4.0 m^3/h due to the active control of the stable flowrate before stopping through the discharge valve. In contrast with the rapid decline of rotating speed in Fig. 3, the flowrate does not drop immediately after non-inertial stopping but only starts a relatively rapid decline after a certain period, that is, a decline in flowrate lag occurs in the early stopping stage. In the five types of stopping, the time for flowrate lag drops is approximately 0.8 s.

The flowrates drop to zero under the five types of stopping states (downtime from short to long), that is, the time required for the fluid to completely stop flowing is approximately 3.984, 8.281, 10.563, 15.531, and 18.625 s. Obviously, the time required for the fluid to completely stop flowing is higher than that for impeller to completely stop rotating. The reason for the lag in flowrate decline is related to the flow inertia of the fluid in the pipeline, that is, after the impeller stops rotating, the flow does not stop immediately due to the flow inertia. Thus, the flow is maintained for a time before it completely stops. Generally, the flow drop curve shows the

characteristics of a linear decline. However, for the slow and superslow states, the flowrate curve shows a sudden drop phenomenon at the end of flow stop. The reason for this phenomenon is that after the flowrate drops, the flow velocity decreases, and the Reynolds number decreases. That is, the flow inertia force decreases, and the viscous force increases, thereby resulting in a sudden drop in flowrate.

Furthermore, the ratio (λ_q) of flowrate attenuation characteristic time (t_q) to the total time (T_q) required to stop the flow is defined to describe the degree of flowrate decline. For the ultra-small-flowrate condition, the flowrate attenuation time ratios (λ_q) of the five types of stopping states (downtime from short to long) are approximately 0.659, 0.669, 0.667, 0.697, and 0.675. The flow attenuation time ratio is slightly greater than 0.632, indicating that the flowrate curve basically conforms to the linear variation characteristics.

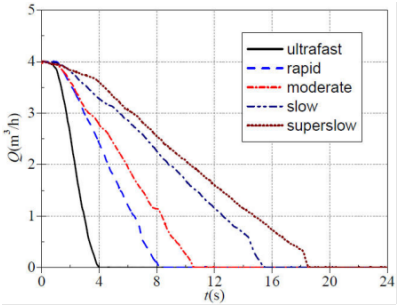

Fig. 4. Instantaneous flowrates (4m^3/h).

Static Pressure at Inlet

During the non-inertial stopping processes, the instantaneous static pressures at the inlet of the pump measured by a WIKA S-10 pressure transmitter are shown in figure 5. It is seen that in the process of non-inertial stoppings, the static pressure change at pump inlet is very drastic, and the evolution law of the static pressures shows obvious differences among different non-inertial stopping states.

For the shut-off condition, in the ultrafast stopping state, the static pressure fluctuates violently, and the maximum and minimum of static pressures are approximately 13.06 and 6.72 kPa, respectively, and tend to be stable at about 4.0 s. In the rapid stopping state, the maximum and the minimum are approximately 10.24 and 8.38 kPa, respectively, and tend to be stable at about 7.0 s. In the moderate stopping state, the maximum and the minimum are approximately 13.01 and 7.60 kPa, respectively. The characteristics of regular fluctuation begin to appear at approximately 10.0 s, and the amplitude decreases gradually. In the slow stopping state, the maximum and the minimum are approximately 9.90 and 8.16 kPa, respectively, and the fluctuation tends to be stable at about 14.0 s. In the superslow stopping state, the static pressure before 8.0 s fluctuates violently, and the maximum and the minimum are about 10.42 and 8.08 kPa, respectively. Then, fluctuation of the static pressure decreases rapidly, and the fluctuation tends to be stable at about 18.0 s.

For the ultra-small flowrate condition, in the ultrafast stopping state, the static pressures fluctuate violently, and the maximum and minimum of the static pressures are approximately 14.46 and 8.36 kPa, respectively. The fluctuation tends to be stable at about 4.0 s. In the rapid stopping state, the maximum and the minimum are approximately 10.10 and 8.56 kPa, respectively, and the fluctuation tends to be stable at about 8.0 s. In the moderate stopping state, the maximum and the minimum are approximately 10.01 and 8.0 kPa, respectively, and the fluctuation decreases gradually at 11.0 s. In the slow stopping state, the maximum and the minimum are approximately 9.86 and 8.25 kPa, respectively, and the fluctuation tends to stabilize at about 16.0 s. In the superslow stopping state, the maximum and the minimum are approximately 9.68 and 7.34 kPa, respectively, and the fluctuation tends to stabilize at about 19.0 s.

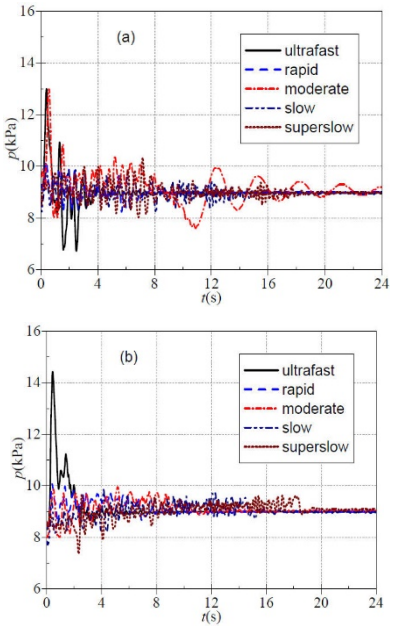

Fig. 5. Instantaneous static pressures at pump inlet (a)Q_i=0 (b)Q_i=4 (m^3/h).

Static Pressure at Outlet

Similarly, the instantaneous static pressures at the pump outlet during non-inertial stopping periods measured by a WIKA S-10 pressure transmitter are shown in Figure 6. Under the shut-off and ultra-small-flowrate conditions, the mean values of measured stable static pressures before stopping are approximately 405.10 and 382.12 kPa, respectively. When the stoppings begin, the rotating speeds of impeller decreases rapidly, and the static pressures at the pump outlet are reduced quickly. For the ultrafast stopping state, the static pressure curves generally presents a linear descent law, and the drop rate begins to decrease at the end of the stopping process.

Theoretically, the static pressure at the pump outlet is proportional to the square of rotating speed. Fig. 6 shows that with the prolongation of downtime, the static pressure curve presents an increasing quadratic parabolic law.

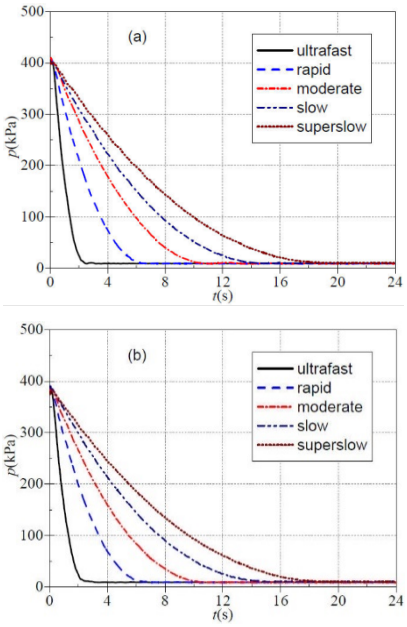

Fig. 6. Instantaneous static pressures at pump outlet (a)Q_i=0 (b)Q_i=4 (m^3/h)

Head Characteristics

It is seen from Fig. 5 that the maximum static pressure at the pump inlet is only 14.46 kPa in all cases. Figure 6 shows that the static pressure at the pump outlet is much larger than these at the pump inlet. Thus, the instantaneous head mainly depends on the change characteristics of the static pressures at the pump outlet. The instantaneous pump heads in the non-stopping processes are shown in Figure 7. Under shut-off and ultra-small-flowrate conditions, the measured mean stable heads before stoppings are approximately 40.41 m and 38.15 m, respectively. Similar to the outlet static pressure, with the prolongation of downtime, the head curve becomes closer to the quadratic parabolic law, which is in line with the general pump fluid dynamics law. This finding indicates that when the similarity law of pump is used to predict the transient performance during the non-inertial stopping process, if the downtime is short, the prediction error will be large due to the large rotating speed and flow acceleration. If the downtime is long, the prediction error will be small due to the small rotating speed and flow acceleration. In other words, the pump similarity law can be applied to the performance prediction of a transient operation process with a long downtime.

For the shut-off state, under the five types of stopping states (downtime from short to long), the heads drop to zero, that is, the time required for the pump head to disappear is approximately 2.906, 6.406, 10.125, 14.437, and 19.329 s. For the ultra-small-flowrate state, the time required for the pump head to disappear is about 3.078, 6.50, 10.297, 14.953, and 20.203 s. Apparently, the required time that the actual head disappears during non-inertial stopping periods is higher than the set time of 1.0, 3.0, 5.0, 7.0, and 9.0 s. Meanwhile, the total time required for head drop shows a slight increase with the increase in stable flowrate before stopping.

Furthermore, the ratio (λ_H) of head attenuation characteristic time (t_H) to the total time (T_H) required to decrease to zero is defined to describe the degree of head decline. For the shut-off state, the head attenuation time ratios (λ_H) of the five types of stopping states (downtime from short to long) are approximately 0.371, 0.414, 0.438, 0.409, and 0.391. For the ultra-small flowrate state, the head attenuation time ratio (λ_H) are approximately 0.341, 0.411, 0.417, 0.392, and 0.375. Whatever, the head attenuation time ratios (λ_H) are less than the rotating speed attenuation time ratios (λ_n), indicating that the head attenuation in the early stage of the stopping process is more rapid than the rotating speed.

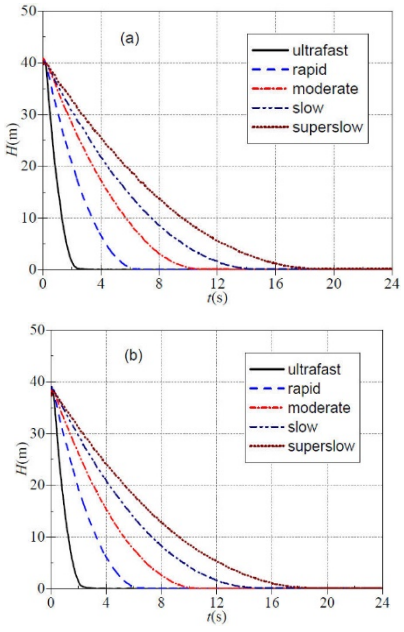

Fig. 7. Instantaneous heads (a)Q_i=0 (b)Q_i=4 (m^3/h)

Shaft Power Characteristics

Through a JC0 torque speed sensor, the instantaneous shaft powers measured in the non-inertial stopping process are shown in figure 8. In this paper, the instantaneous rotating speed and the instantaneous shaft power are measured by the same sensor. Thus, both of them have similar evolutionary characteristics with time. That is, for the shut-off state and under the five types of stopping states (downtime from short to long), the time required for the instantaneous shaft powers to decline to zero is approximately 1.578, 3.312, 5.219, 7.203, and 9.141 s. For the ultra-small-flowrate state, the total time

required for the instantaneous shaft powers to decline to zero is approximately 1.531, 3.343, 5.203, 7.219, and 9.109 s.

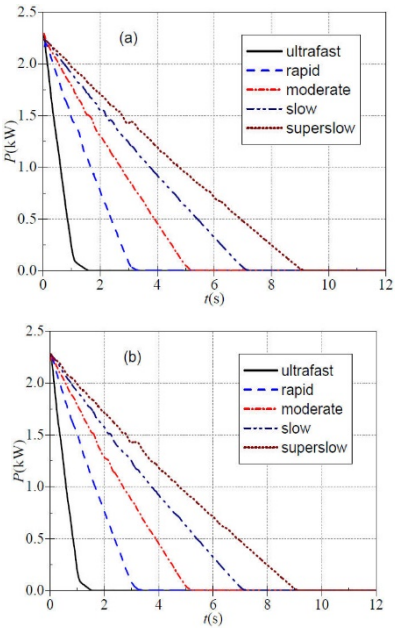

Fig. 8. Instantaneous shaft powers (a)Q_i=0 (b)Q_i=4 (m^3/h)

In this paper, the ratios (λ_P) of the attenuation characteristic time of shaft power (t_P) to the total time required for the shaft powers to fall to zero (T_P) is the same as the rotating speed attenuation time ratio (λ_n). That is, for the shut-off state, under the five types of stopping conditions, the shaft power attenuation time ratios (λ_p) are also approximately 0.463, 0.607, 0.623, 0.623, and 0.629. For the ultra-small-flowrate state, the corresponding shaft power attenuation time ratios (λ_P) are approximately 0.475, 0.595, 0.625, 0.620, and 0.626.

Under the shut-off and ultra-small-flowrate conditions, the measured mean stable shaft powers before stopping are approximately 2.241 and 2.254 kW, respectively. That is, shaft power shows an increasing trend with the increase in stable flowrate before stopping, which conforms to the general hydrodynamic law of centrifugal pumps.

A comparison of flowrate attenuation time ratio (λ_Q), head attenuation time ratio (λ_H), and shaft power attenuation time ratio (λ_P) shows that the relationship among the three parameters is: $\lambda_H<\lambda_P<\lambda_Q$, indicating that during the non-inertial stopping process, the parameters are affected by the importance order of the head, shaft power, and flowrate.

DIMENSIONLESS ANALYSIS

In reference (Tsukamoto, 1982), two dimensionless flowrate and dimensionless head coefficients were used to reveal the transient characteristics during the start-up process to eliminate the effect of variable rotating speed during start-up. On this basis, a dimensionless shaft power coefficient is introduced in the current study to deeply describe the transient characteristics in the non-inertial stopping process. These three coefficients exclude the effect of rotating speed change, that is, they have nothing to do with rotating speed. The three parameters are defined as follows:

$$\begin{cases} \phi(t) = Q(t) / \pi D_2 b_2 u_2(t) \\ \psi(t) = 2gH(t) / u_2^2(t) \\ \Phi(t) = P(t) / \rho D_2^2 u_2^3(t) \end{cases} \quad (1)$$

where $u_2(t)$ is the instantaneous circumference velocity at the impeller outlet, and its expression is $u_2(t)=\pi D_2 n(t)/60$. Figures 9, 10, and 11 present the time evolution process of instantaneous dimensionless flowrate, head, and shaft power during the non-inertial stopping process, respectively.

The calculating results show that the dimensionless flowrate, head, and shaft power coefficients have similar evolutionary characteristics. That is, at the beginning of the non-inertial stopping process, the three coefficients have respective minimum values. Then, they approximately maintain respective constant values during most of the stopping process. At the end of the stopping process, the three coefficients rapidly increase to the respective maximum values.

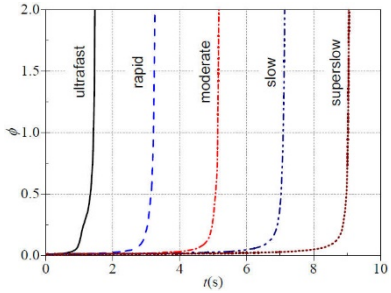

Fig. 9. Instantaneous dimensionless flowrates ($4m^3$/h)

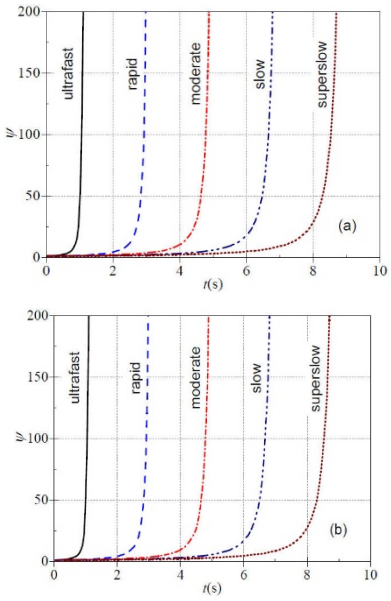

Fig. 10. Instantaneous dimensionless heads (a)Q_i=0

(b)Q_i=4 (m^3/h)

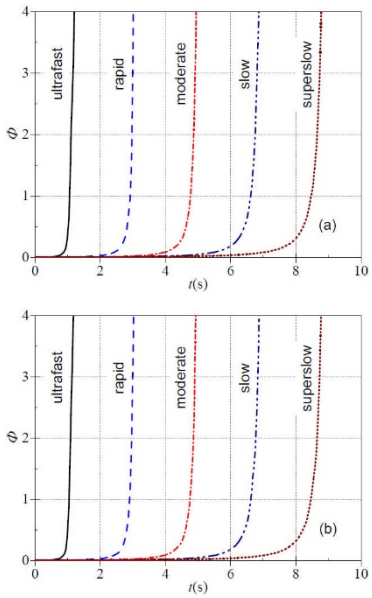

Fig. 11. Instantaneous dimensionless shaft powers (a)Q_i=0 (b)Q_i=4 (m^3/h)

DISCUSSIONS

To better reveal the transient characteristics of pump model during non-inertial stopping process, Figure 12 shows the instantaneous head-flowrate curves in the process of non-inertial stopping. Meanwhile, the head-flowate curve based on the similarity law of pump is also given. For the ultrafast stopping state, the head drops rapidly as the flowrate decreases. When the flowrate drops to a certain extent, the drop rate of head decreases significantly and shows a trend of slow descent to zero. Comparing with the ultrafast stopping, the droping rate of the head decreases significantly in the rapid stopping state. With the prolongation of downtime, the drop rate of head decreases, and the instantaneous head-flowrate curve becomes increasingly consistent with the head-flowrate curve based on the similarity law. The similarity law of pump becomes increasingly suitable for the performance prediction in the process of non-inertial stopping state with the decrease in rotating speed acceleration and flowrate acceleration in the stopping process. The instantaneous head-flowrate curves are basically the same, especially for slow and superslow stopping states.

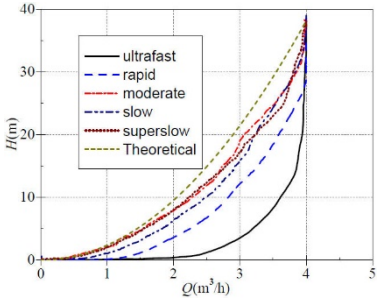

Fig. 12. Instantaneous head-flowrate curve (4m^3/h)

CONCLUSIONS

Under the shut-off and ultra-small-flowrate conditions, the transient performance of pump during the non-inertial stopping process is experimentally investigated in this study, and the effect of downtime on non-inertial stopping performance is examined. The transient characteristics of the pump model during non-inertial stopping process are deeply revealed with the aid of three dimensionless parameters.

(1) In the non-inertial stopping process, the extent to which parameters are affected is from heavy to light in the order of head, shaft power, and flowrate.

(2) At the beginning of non-inertial stopping process, the dimensionless flowrate, head, and shaft power coefficients have minimum values and are almost unchanged during the stopping process. At the end of the stopping process, the three coefficients increase rapidly to the maximum values. The transient behaviour of the pump model in the non-inertial stopping process mainly occur at the end of non-inertial stopping process.

(3) The shorter the downtime is, the more prone it is to rotating speed drop delay at the end of the non-inertial stopping process.

(4) In the early stage of the non-inertial stopping process, a common phenomenon of flowrate drop lag is observed. The longer the downtime is, the more likely the flowrate curve is to have a flow drop phenomenon at the end of the stopping flow. The flow inertia of fluid stored in the impeller and pipelines makes the flow stop longer.

(5) The total time required for head drop shows a slight increase with the increase in stable flowrate before stopping. The head curve becomes closer to the quadratic parabolic law with the prolongation of downtime. The similarity law of pump can be applied to the performance prediction in a transient operating process with a long downtime.

ACKNOWLEDGMENT

The research was financially supported by the National Natural Science Foundation of China (Grant No.51876103, No. 51976202).

REFERENCES

Chen, W., Ke, X.W. and Wu, D.Z. "Analysis on transient performance of mixed flow pump during stopping period," *FLUID MAC*, Vol. 34, No. 2, pp. 1-4 (2006). (in Chinese with English abstract)

Dazin, A., Caignaert, G. and Bois, G. "Transient behavior of turbomachinery: applications to radial flow pump startups," *J FLUID ENG-T ASME*, Vol. 129, No. 11, pp. 1436-1444 (2007).

Duplaa, S., Coutier-Delgosha, O. and Dazin, A. "Experimental study of a cavitating centrifugal pump during fast startups," *J FLUID ENG-T ASME*, Vol. 132, No. 2, pp. 1-12 (2010).

Gao, H., Gao, F. and Zhao, X.C. "Transient flow analysis in reactor coolant pump systems during flow coastdown period," *NUCL ENG DES*, Vol. 241, pp. 509-514 (2011).

Gao, H., Gao, F, and Zhao, X.C. "Analysis of reactor coolant pump transient performance in primary coolant system during start-up period," *ANN NUCL ENERGY*, Vol. 54, pp. 202-208 (2013).

Lefebvre, P.J. and Barker, W.P. "Centrifugal pump performance during transient operation," *J FLUID ENG-T ASME*, Vol. 117, NO. 2, pp. 123-128 (1995).

Li, Z.F., Wu, D.Z. and Wang, L.Q. "Numerical simulation of the transient flow in a centrifugal pump during starting period," *J FLUID ENG-T ASME*, Vol. 132, No. 8, pp. 1-8 (2010).

Liu, J.T., Li, Z.F. and Wang, L.Q. "Numerical simulation of the transient flow in a radial flow pump during stopping period," *J FLUID ENG-T ASME*, Vol. 133, No. 11, pp.1-7 (2011).

Rong, W.H., Tanaka, K. and Ootsu, T. "Analysis of Pump Transient during Starting/Stopping Periods by Bond Graph," *THE JAP SCI OF MEC ENG*, Vol. 62, pp. 677-683 (1996).

Tanaka, T. and Tsukamoto, H. "Transient behavior of a cavitation centrifugal pump at rapid change in operating conditions-part2: transient phenomena at pump startup/shutdown," *J FLUID ENG-T ASME*, Vol. 121, No. 4, pp. 850-856 (1999).

Tanaka, T. and Tsukamoto, H. "Transient behavior of a cavitation centrifugal pump at rapid change in operating conditions-Part1: Transient phenomena at opening/closure of discharge valve," *J FLUID ENG-T ASME*, Vol. 121, No. 4, pp. 841-849 (1999).

Thanapandi, P. and Prasad, R. "A quasi-steady performance prediction model for dynamic characteristics of a volute pump," *CSEE J POWER ENERGY*, Vol. 208, No. 1, pp. 47-58 (1994).

Thanapandi, P. and Prasad, R. "Centrifugal pump transient characteristics and analysis using the method of characteristics," *INT J MECH SCI*, Vol. 37, No. 1, pp. 77-89 (1995).

Tsukamoto, H. and Ohashi, H. "Transient characteristics of a centrifugal pump during startup period," *J FLUID ENG-T ASME*, Vol. 104, No. 1, pp. 6-13 (1982).

Tsukamoto, H., Matsunaga, S. and Yoneda, H. "Transient characteristics of a centrifugal pump during stopping period," *J FLUID ENG-T ASME*, Vol. 108, No. 4, pp. 392-399 (1986).

Wang, X.L., Yuan, S.Q. and Zhu, R.S. "Transient hydraulic characteristics study on nuclear reactor coolant pump during stopping period," *ATO ENER SCI AND TECH*, Vol. 47, No. 3, pp. 364-370 (2013). (in Chinese with English abstract)

Wu, D.Z., Wu, P. and Li, Z.F. "The transient flow in a centrifugal pump during the discharge valve rapid opening process," *NUCL ENG DES*, Vol. 240, No. 12, pp. 4061-4068(2010).

Wu, D.Z., Wu, P. and Yang, S. "Transient characteristics of a close-loop pipe system during pump stopping periods," *J PRESS VESS-T ASME*, Vol. 136, No. 2, pp.1-8 (2014).

Wu, G.W., Jin, M. and Li, Y.Z. "Primary pump coast-down characteristics analysis in lead cooled fast reactor under loss of flow transient," *ANN NUCL ENERGY*, Vol. 103, pp. 1-9 (2017).

Wu, P., Wu, D.Z. and Li, Z.F. "Study of transient flow in centrifugal pump during flow impulsively increase process," *J OF ENF THER*, 2010, Vol. 31, No. 3, pp. 419-422 (2010). (in Chinese with English abstract)

Zhang, Y.L., Zhu, Z.C. and Cui, B.L. "Numerical simulation of unsteady flow in centrifugal pump during stopping period," *J ENG THERMOPHYS-RUS*, Vol. 33, No. 12, pp. 2096-2099 (2012). (in Chinese with English abstract)

Zhang, Y.L., Li, Y. and Zhu, Z.C. "Computational analysis of centrifugal pump delivering solid-liquid two-phase flow during startup period," *CHIN J MECH ENG-EN*, Vol. 27, No.1, pp. 178-185 (2014a).

Zhang, Y.L., Xiao, J.J. and Cui, B.L. "Study on transient behavior in a prototype centrifugal pump during rapid regulating flow rate," *TRAN OF THE CHIN SOCI OF AGRI ENG*, Vol. 30, No. 11, pp. 68-75 (2014b). (in Chinese with English abstract)

Zhang, Y.L., Zhu, Z.C. and Li, W.G. "Experiments on transient performance of a low specific speed centrifugal pump with open impeller," *CSEE J POWER ENERGY*, Vol. 230, No. 7, pp. 648-659 (2016).

Zhang, Y.L., Wang, C.F, and Zhang, C.L. "Numerical study on transient stopping characteristics of the first stage impeller of a multistage pump," *J OF MEC& ELEC ENG*, Vol. 34, No. 1, pp. 10-17 (2017a). (in Chinese with English abstract)

Zhang, Y.L., Zhu, Z.C, and Dou, H.S. "Numerical Investigation of Transient Flow in a Prototype Centrifugal Pump during Startup Period," *INT*

J TURBO JET ENG, Vol. 34, No. 2, pp. 167-176 (2017b).

Zhang, Y.L., Zhu, Z.C, and Li, W.G. "Effects of viscosity on transient behaviour of a low specific speed centrifugal pump in starting and stopping periods," *INT J FLUID MEC RESEARCH*, Vol. 45, No. 1, pp. 1-20 (2018a).

Zhang, Y.L., Zhu, Z.C, and Li, W.G. "Hydraulic performance of low specific-speed centrifugal pump with compound impeller during stopping period," *TRANS OF THE CHI SOCI OF AGRI ENG*, Vol. 34, No. 12, pp. 95-103 (2018b). (in Chinese with English abstract)

Zou, X.L., Zhou, T. and Zhang, G.Y. "Analysis of core blockage scenarios during pump shutdown accidents for small size lead-cooled fast reactor using RELAP5-HD," *PROG NUCL ENERG*, Vol. 111, pp. 205-210 (2019).

NOMENCLATURE

λ_n the ratios of the attenuation characteristic time of rotating speed

t_n the attenuation characteristic time

T_n the total time required for the impeller to stop

λ_q the ratio of flowrate attenuation characteristic time to the total time required to stop the flow

t_q flowrate attenuation characteristic time

T_q the total time required to stop the flow

λ_H the ratio of head attenuation characteristic time to the total time required to decrease to zero

t_H head attenuation characteristic time

T_H the total time required to decrease to zero

λ_P the ratios of the attenuation characteristic time of shaft power to the total time required for the shaft powers to fall to zero

t_P the attenuation characteristic time of shaft power

T_P the total time required for the shaft powers to fall to zero

$u_2(t)$ the instantaneous circumference velocity at the impeller outlet

自吸泵特殊工况非惰轉特性實驗

趙燕娟
衢州職業技术學院

張玉良
衢州學院機械工程學院

張玉良 周鳳林
湖南工業大學機械工程學院

摘 要

本文對自吸泵關死點工况和超小流量工况進行了非惰轉過程的效能實驗研究，研究了停機時間對非惰轉效能的影響。同時借助於無量綱分析方法揭示了非惰轉過程中的瞬態特性。研究發現：停機時間越短，非惰轉過程末期越容易出現轉速下降延遲現象。停機時間越長，非惰轉過程末期越容易出現流量突降現象。非惰轉過程初期普遍存在流量下降滯後現象。三個無量綱係數在非惰轉過程初期均具有極小值，隨後近似保持不變，在停機末期迅速上升至極大值。非惰轉過程中參數受影響的程度由重到輕的順序為揚程、軸功率和流量。泵相似定律可適用於停機時間較長的瞬態操作過程效能預測。